Lasers in Manufacturing Conference 2017

Laser surface texturing of natural stones

A. Chantada, J. Penide, P. Pou, A. Riveiro, J. del Val, F. Quintero, R. Soto, F. Lusquiños, J. Pou*

Applied Physics Department, University of Vigo, EEI, Lagoas-Marcosende, Vigo, E- 36310, Spain

Abstract

In recent years, controlling the wetting features of materials is attracting much interest in applications related to surface cleaning. The phenomenon of surface cleaning is closely related to morphology, and chemistry of surfaces. These characteristics can be modified by subjecting materials to surface treatments. One of the most promising techniques aiming to modify surface features is the laser texturing. In such a way, it is possible to achieve the surface properties leading to the desired wettability in an accurate manner, and with minor contamination.

In this work, the wetting features of Zimbabwe black granite, a middle-to-fine-grained natural stone commonly employed as countertops in kitchens and bathrooms, are modified by laser surface texturing. The main aim is to increase its hydrophobic degree so as to reduce the attachment of contaminants on the surface. For such purpose, two laser sources (λ = 1064 and 532 nm) were employed. The effect of the laser wavelength, along with other processing parameters, were evaluated. In this way, those parameters resulting in the highest hydrophobic degree were identified. It was found that the 532 nm laser wavelength was the most effective one in this regard. Furthermore, the morphology resulted from the laser surface texturing was found to be the principal phenomenon governing the wettability modifications, as the chemical composition remained virtually unaltered after treatment.

Keywords: laser surface texturing, wettability, roughness, natural stone, design of experiments

1. Introduction

Among the wide range of natural stones used currently in construction industry, granite represents the greatest part of the production (Stone sector, 2016). This is a crystalline igneous rock composed essentially of quartz, feldspars and mica. Its use as building material is not only restricted for outdoor constructions but

* Corresponding author. Tel.: +34-986-812216;
E-mail address: jpou@uvigo.es

also for countertops in the domestic environment, such as kitchens and bathrooms. In this case, surface contamination due to the presence of bacteria may result in disease transmission (Scott et al., 1982, Jensen et al., 2013). The contamination is a superficial problem that depends to a large extent of the wettability of the surface, because this parameter controls the bacterial adhesion (Kumar and Pranhu, 2007). The correlation between the degree of wettability of a substrate and the number of microbial cells attached has been already established, resulting in an inversely proportional relationship between them (Li and Logan 2004). Several authors like Nosonovsky et al., 2009 or Ragesh et al., 2014 have establish that by means of the use of superhydrophobic surfaces the elimination of the superficial contamination can be achieved by means of the self-cleaning phenomenon. This phenomenon, as is observed in hydrophobic surfaces by Bhushan and Jung, 2011, is based on the rolling of the liquid droplets which trap contaminant particles along the surface leading to the removal of the undesirable contamination. Laser surface texturing is a well-known method to modify the wettability of a great range of materials, as is pointed by different authors (Kietzig et al., 2011, Vorobyev and Guo, 2013, Riveiro et al., 2014, Ta et al., 2015). Furthermore, the research conducted by Wu et al., 2009 shows that it offers advantages over other chemical techniques (e.g. silanization of post-textured surfaces), such as its higher processing rate, or the fact that there is no need of using prior or subsequent coatings (Kietzig et al., 2009, Rukosuyev et al., 2014). Also, the laser treated resulting surface is free of contaminants without change in the bulk properties of the material, fact that adds value to this technique. The studies of Jadgheesh et al., 2011, Riveiro et al., 2012 and Wang and Bai, 2015 have demonstrated that the laser texturing can be applied to different materials because is based on the absorption of the radiation by the matter, but to the best of author's knowledge, it has not been applied to natural stones yet.

In the present paper, laser surface texturing of Zimbabwe black granite is analyzed. The effect of the laser processing parameters on the wettability and surface roughness was performed for two different wavelengths (λ = 1064 and 532 nm). The aim of this work is the study of the effect of processing parameters on the wettability and roughness of granite with the aim of obtaining hydrophobic granite surfaces. This will make possible the control of contaminants and the presence of bacteria on the surface of these materials. The influence of the laser processing parameters (laser power, scanning speed, pulse frequency and spot overlapping) on the treated surfaces of granite was analyzed by means of statistically planed experiments.

2. Materials and methods

2.1. Sample material

The base material used to carry out all the experiments was Zimbabwe black granite, in form of square polished slabs samples with dimensions of 5 cm (length) x 5 cm (width) x 2 cm (height). The Zimbabwe black granite is a middle-to-fine grained natural stone. Belongs to the family of igneous rocks and is characterized by exhibiting a deep black appearance and small bright areas due to the presence of quartz in its morphology. Is principally composed of quartz, calcium-rich plagioclase feldspar and orthopyroxenes, and also presents small proportions of biotite and diopsides.

2.2. Experimental system

Laser surface treatments were performed using a diode end-pumped Nd:YVO_4 (Rofin-Sinar PowerLine E) laser source, emitting in TEM_{00} laser beam mode at two different wavelengths; the first one at 1064 nm with $M^2 < 1.3$ and 20 ns of pulse duration and second one at 532 nm with $M^2 < 1.5$ and 14 ns of pulse duration. For both wavelengths the laser beam was focused onto de surface of the granite sample by an optical system composed of a pair of a dual-axis scanning galvo system and a F-Theta lens, with a focal length of 211 mm for

λ=1064 nm (spot size = 70 µm) and 365 mm for λ=532 nm (spot size = 60 µm). Moreover, laser surface treatments were performed in air at atmospheric pressure. In order to identify the key processing parameters of the process that statistically influence (*p-value* < 0.05), a 2^4 Full Factorial Design (FFD) of experiments was elaborated on the dependent response variables, the average roughness of the treated areas and the water contact angle. Based on previous works (Riveiro et al., 2014) the processing parameters selected for this case of study were the laser power (*P*), the scanning speed (*v*), the pulse frequency (*f*) and the pass overlapping (*s*). Each laser processing parameter, with its high "+" and low "-" levels, are shown in Table 1. An analysis of the variance (ANOVA) was performed to find out which are the most statistically significant factors on the response variables. Then, a linear regression model was calculated to determine a statistical model between the response variables.

Table 1. *Processing parameters with corresponding levels for the 2^4 Full Factorial Design.*

Wavelength, λ (nm)	Laser Power, P (kW)		Processing speed, v (mm/s)		Pulse frequency, f (kHz)		Overlapping, s (%)	
	+	-	+	-	+	-	+	-
1064	3.3	1.5	20	1	30	20	50	0
532	1.4	0.8	20	1	30	20	50	0

2.3. Sample characterization

The surfaces of the laser treated samples were inspected in frontal view to the laser treated area by a Phillips XL-30 scanning electron microscope (SEM) system equipped with an energy dispersive X-ray spectroscope (EDS EDAX PV9760) in order to obtain the semi-quantitative chemical composition. Moreover, selected samples were analyzed by means of X-ray Diffraction (XRD) using a SIEMENS D-500 diffractometer to determine structural changes on the surface of the samples. Also, a Bruker Dektak XT surface profiler was used to obtain the surface morphology of the selected treated areas, by means of 2D height-maps, to evaluate the effect of different treatments on the surface damage of the samples.

The average roughness value (Ra) of the treated areas was obtained by the mean value of 5 measurements in each treated area, obtained by means of a TESA-Rugosurf 10G surface profilometer.

The water contact angle (θ) was measured using distilled water by means of the sessile drop technique according to the recommendations given by the UNE-EN 828:2013 standard.

3. Results and discussion

3.1. Selection of laser surface texturing parameter.

Regarding to the roughness analysis, the average roughness both for 1064 and 532 nm wavelengths show a similar behaviour as is derived from the analysis of the 2^4 FFD. In this case, the scanning speed and particularly the laser power are the most statistically significant factors on the roughness of the surfaces after the laser treatments, while the effect of the pulse frequency and overlapping on the surface roughness is much lower in comparison and can be neglected in all cases. Fig 1 shows the response surfaces for the average roughness (plotted only terms through order 1), based on the following linear regression equations:

$$R_a(\mu m) = -1.077 + 2.290P - 7.437x10^{-2}v + 5.464 \cdot 10^{-2}f - 6.475 \cdot 10^{-5}s \ (for\ \lambda = 1064\ nm) \qquad (1)$$

$$R_a(\mu m) = 0.938 + 5.613P - 0.122v + 0.124f - 0.013s\ (for\ \lambda = 532\ nm) \quad (2)$$

As expected, the increment of the laser power tends to increase the average roughness both for 1064 and 532 nm laser radiation wavelengths. A possible explanation could be that an increase on the laser power leads to a larger amount of energy deposited on the surface, and therefore a more pronounced melting. Conversely, the increment of the scanning speed reduces the average roughness of the surface owing to the reduction of the energy deposition per unit of length, reducing the capacity of the laser beam to damage the surface of the sample. These behavior in the roughness is in agreement with those found in literature for polymers (Riveiro et al., 2014, Riveiro et al, 2016) and metals (Razi et al., 2016).

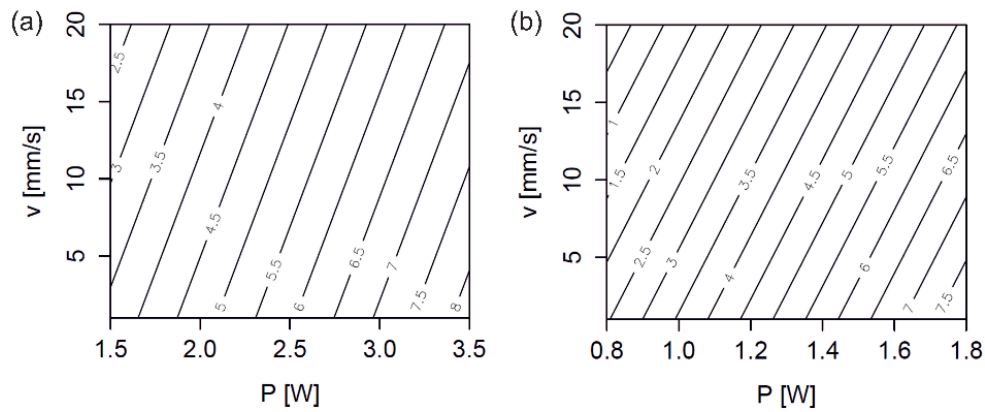

Fig. 1. Contour plot of the average roughness Ra (μm) versus laser power and scanning speed during the laser surface treatment for (a) 1064 nm and (b) 532 nm laser wavelengths.

Regarding to the water contact analysis, the 2^4 FFD reveals a similar result of tendency for both laser radiation wavelengths. The most relevant factors on the wettability of the surface after the laser treatment are again laser power and scanning speed. However, in the case of 1064 nm, the spot overlapping is also a significant factor influencing the water contact angle compared with the 532 nm case. The pulse frequency can be neglected in all cases. The response surfaces (plotted in Figure 2 including only terms up through order 1) can be calculated by the following linear regression equations:

$$\vartheta(^o) = 59.116 - 10.001P + 1.869v - 0.428f - 0.267s\ (for\ \lambda = 1064\ nm) \quad (3)$$

$$\vartheta(^o) = 51.610 + 31.910P - 1.308v + 0.784f - 0.009s\ (for\ \lambda = 1064\ nm) \quad (4)$$

As can be observed in Fig 2, the influence of the scanning speed in the water contact angle for the treatments under 1064 nm is stronger than for 532 nm laser radiation. The highest values of water contact angle are achieved in the case of laser treatments with 532 nm wavelength, and having the lowest values of this response variable for the case of 1064 nm laser radiation. For both laser wavelengths, as the laser power increase and the scanning speed decreases the water contact angle is reduced, increasing the wettability of the surface. This tendency is in line with the increase of the average roughness after the laser treatment (Fig 2). This phenomenon agrees with the Wenzel model proposed by Wenzel, 1936, which indicates that the endowment of roughness on a surface increases the inherent wetting behaviour of the precursor material, turning, in this case, the Zimbabwe black granite more wettable (contact angle of the original surface of 57.86^o).

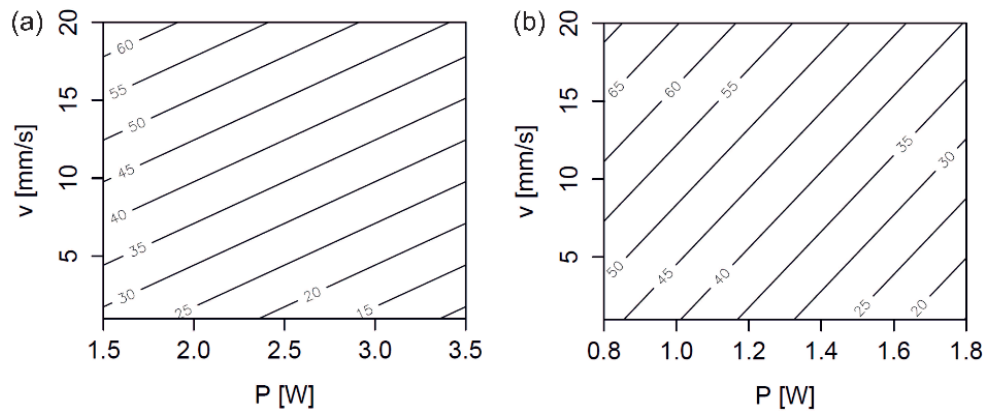

Fig. 2. Contour plot of the water contact angle θ (º) versus laser power and scanning speed during the laser surface treatment for (a) 1064 nm and (b) 532 nm laser wavelengths.

According to this theory, if the original surface prior to the surface treatment is hydrophilic, the surface after being textured will become more hydrophilic. In such a case, as the roughness increases, the water droplet fills the grooves of the rough surface, increasing the interface area water-rough surface. This, in turn, increases the interfacial tension solid-liquid, which leads to a decrease in the water contact angle by solving the equilibrium equation of interfacial tensions of the wetting model (Young, 1805). Indeed, Fig **Fehler! Verweisquelle konnte nicht gefunden werden.**3 reveals that the lowest contact angles are obtained when the average roughness achieves the highest values, which is consistent with the aforementioned explanation.

However, as can be observed in Fig 3, when the values of Ra are below 3 µm (1064 nm) or 2.5 µm (532 nm), the water contact angle shows values above the untreated surface of Zimbabwe black granite contact angle, reaching values up to 76.77º and 83.99º for 1064 and 532 nm laser wavelengths, respectively. An explanation of this phenomenon could be that in the case of large grooves the water can penetrate inside the grooves and then the wettability is increased. However, when the grooves are small enough the water cannot penetrate in the grooves due to the surface tension of the drop, and therefore, the surface presents gaps of air that tend to increase the water contact angle (Young, 1805, Cassie et al., 1944).

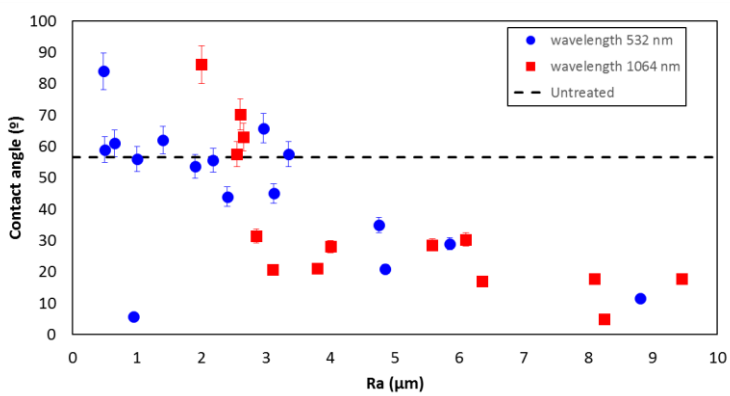

Fig. 3. Values of the water contact angle θ (º) corresponding to each value of average roughness Ra (µm) of the untreated surface and after the laser surface treatments for 1064 and 532 nm wavelengths.

As a general rule, the evolution of the water contact angle with the average roughness is similar under 1064 and 532 nm laser wavelengths, as the average roughness increases, the water contact angle decreases. Results suggest that both laser wavelengths are suitable to increase the hydrophobic degree of the Zimbabwe black granite. Specifically, it was possible to increase the water contact angle in a 33 % and 45 % comparing to that of the untreated surface, when processing under 1064 and 532 nm laser wavelengths respectively. It can be deduced that the 532 nm is more effective to increase the hydrophobic degree of the surface, and therefore, to reduce the attachment of contaminants on the surface.

Optical observation of the surfaces after processing at λ = 1064 nm reveals an irregular texturing, leading to the highest contact angles. The molten material can be detected by the lighter areas in comparison with the darker background of the granite surface. This phenomenon is confirmed by the different height patterns revealed by interferometric profilometry (Fig 4b), where the red areas (peaks in the sample) correspond to the molten material, while the blue areas (valleys found in the sample) correspond to areas with material removal. The unique laser affected areas seen in Fig 4c correspond to biotite.

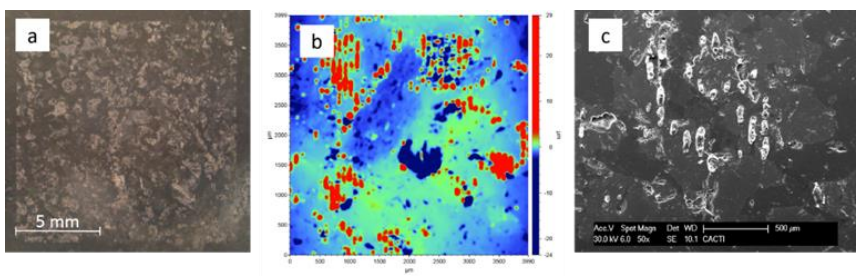

Fig. 4. (a) Micrograph of the granite surface after the laser treatment with 1064 nm wavelength which leads to the highest water contact angle, (b) interferometric profilometry of an area of 4 x 4 mm^2 and (c) SEM image showing the melting of biotite of an area treated with the same laser parameters (processing parameters: P = 1.5 W, v = 20 mm/s, f = 20 kHz, s = 0 %).

In the case of laser surface treatment at λ = 532 nm (leading to the highest contact angle, *Ra* = 0.489 µm and $\vartheta = 83.99^{o}$), Fig 5 shows again that the appearance of the textured surface is irregular (Fig 5a-b). The 2-D map obtained by the interferometric profilometry (Fig 5b) reveals lower height patterns compared to those for the laser treatment with 1064 nm wavelength. This is also reflected in the lower value of average roughness of the surface shown in Figure 4 (*Ra* = 0.489 µm for λ = 532 nm) compared to that in Figure 5 (*Ra* = 2.036 µm for λ = 1064 nm). The irregularity in the texturing is attributed to the different radiation absorption features at 532 nm of the grains of the Zimbabwe black granite.

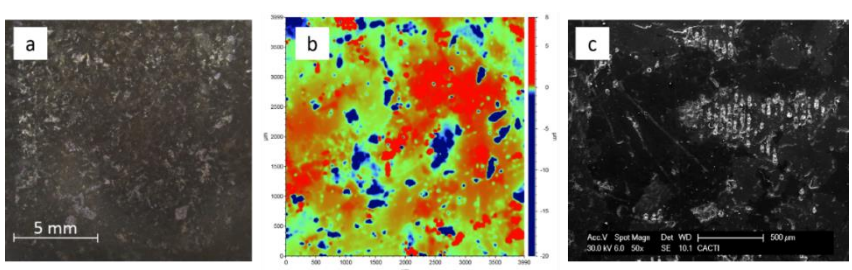

Fig. 5. (a) Micrograph of the granite surface after the laser treatment with 532 nm wavelength which leads to the highest water contact angle, (b) interferometric profilometry of an area of 4 x 4 mm^2 and (c) SEM image showing the melting of biotite of an area treated with the same laser parameters (processing parameters: P = 0.8 W, v = 20 mm/s, f = 30 kHz, s = 50 %).

3.2. X-ray and EDS analysis

Several analysis by means of X-ray diffraction (XRD) were performed of the surface morphology of Zimbabwe black granite sample before and after laser treatments. In such a way, modifications on the crystalline phases of the natural stone surface after laser surface texturing can be detected (Pou et al., 2003, Riveiro et al., 2016).

The partial amorphization of several crystalline phases of the Zimbabwe black granite surface after laser treatments with 1064 and 532 nm wavelengths can be observed in Fig 6. Results from XRD analysis put forward that the surface irradiated with 1064 nm is the most affected one, since, except in the case of certain crystallographic directions of quartz grains, which just get partially amorphidized, the rest of the components become totally amorphous. In the case of 532 nm wavelength, a partial amorphization occurs in the case of some crystals but to a lesser extent compared to the treatment under 1064 nm radiation. Again, several crystallographic directions of quartz and, also, of pyroxene grains become only partially amorphous in the case of the surface irradiated with 532 nm wavelength. In this case, the proportion of crystalline phases of pyroxenes increases as compared to the original surface, which means that there exists a lesser amorphization of pyroxene crystals than in any other crystal. For the same wavelength, there was almost no amorphization of crystalline phases of biotite and in the case of diopside, its crystallographic structure becomes practically amorphous after the laser treatment. In the case of feldspar grains, their structure becomes totally amorphous after the laser treatment with 532 nm laser wavelength.

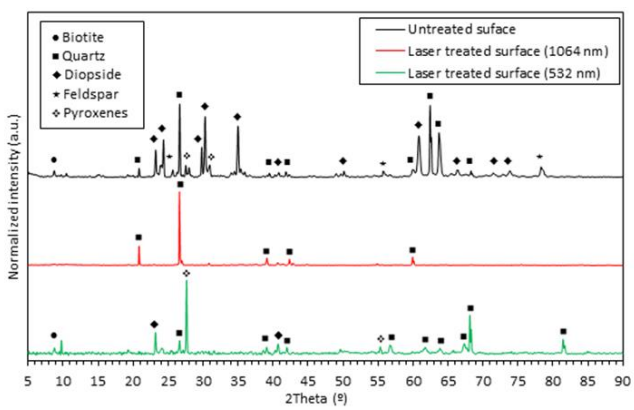

Fig. 6. XRD spectra of the original surface, the laser treated surface with 1064 nm (processing parameters: P = 3.3 W, v = 1 mm/s, f = 30 kHz, s = 50 %) and the laser treated surface with 532 nm (processing parameters: P = 1.4 W, v = 1 mm/s, f = 20 kHz, s = 50 %) showing the amorphization of the material after laser surface texturing.

SEM-EDX analysis shown in Fig 7 confirmed that the observed molten material corresponds to biotite, remaining the rest of the grains unaltered after the laser treatment. This phenomenon may be attributed to the high radiation absorptivity of the biotite at this laser wavelength (Rodrigues et al. 2014, Karickhoff and Bailey, 1973), which makes the biotite melt at low laser fluences. Regarding the chemical composition of the Zimbabwe black granite, the EDS (Fig 7) after and before the laser treatment are practically identical, with a slight decrease in the proportion of Fe and K with respect to the other chemical components due to the effect of the laser treatment. This means that the variations in the wettability of Zimbabwe black granite can

be solely due to the modifications in the surface morphology, supporting the explanation aforementioned for the changes in the water contact angles.

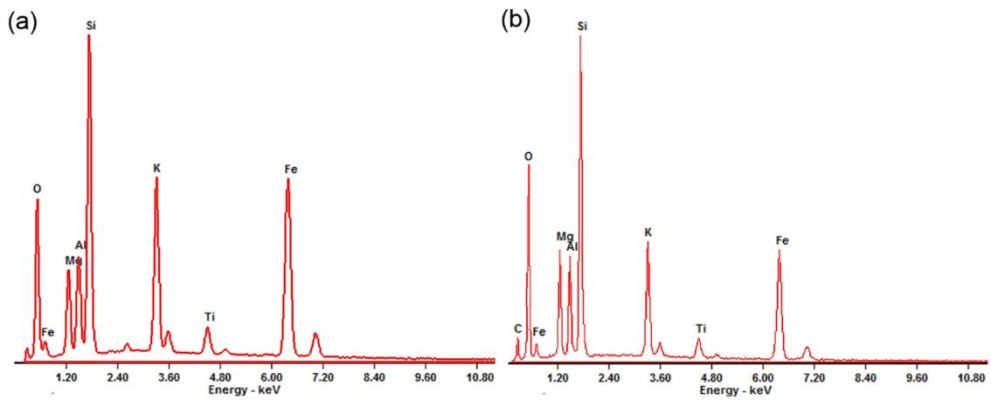

Fig. 7. EDX spectrum of the biotite of Zimbabwe black granite (a) before and (b) after the laser treatment with λ=532 nm (processing parameters: P = 0.8 W, v = 20 mm/s, f = 30 kHz, s = 50 %).

4. Conclusions

The effect of laser processing parameters on the average roughness and water contact angle (parameters directly related to the wettability) of Zimbabwe black granite surface, treated with 1064 and 532 nm laser wavelengths, was statistically assessed by means of a Full Factorial Design. Results indicate that both laser wavelengths are suitable to tailor the wettability of Zimbabwe black granite. Laser power and scanning speed were the most statistically affecting factors. Furthermore, for any of the laser wavelengths employed, as the energy deposition on the surface of the samples increases, the average roughness increases and the water contact angle decreases. However, as the average roughness reduces below 2.5-3 µm, the water contact angle becomes higher than that for the original surface, increasing the hydrophobic degree. This phenomenon may be caused by the formation of air pockets in the grooves of the rough surface below the water droplet when they are sufficiently small. An increase in the water contact angle of 33 % and 45 %, by means of laser treatments with 1064 and 532 nm laser wavelengths respectively, was achieved. It was found that the 532 nm laser wavelength was the most effective one to increase the hydrophobic degree of the surface, and therefore, to reduce the attachment of contaminants on the surface.

XRD analyses reveal partial amorphization of certain crystalline phases both for 1064 and 532 nm wavelength depending on their optical absorptivity features and melting points. SEM-EDX analyses and interferometric spectroscopy images show irregularities in the laser affected surface zones due to the different absorptivity of the grains of Zimbabwe black granite, being the biotite the most affected grain by the laser treatment both for 1064 and 532 nm wavelength with fluences leading to the highest contact angles.

In summary, it was demonstrated the capabilities of the laser surface texturing to enhance the hydrophobic degree of the Zimbabwe black granite.

Acknowledgements

The authors wish to thank the technical staff from CACTI (University of Vigo) for their help with sample characterization. This work was partially supported by Government of Spain (MAT2015-71459-C2-P) and Xunta de Galicia (ED431B 2016/042, POS-A/2013/161, ED481B 2016/047-0).

References

Bhushan, B., Jung, Y.C., 2011. Natural and biomimetic artificial surfaces for superhydrophobicity, self-cleaning, low adhesion, and drag reduction, Progress in Materials Science 56, p. 1–108.

Cassie, A.B.D., Baxter, S., 1944. Wettability of porous surface, Transactions of the Faraday Society 40, p. 546–551.

Jagdheesh, R., Pathiraj, B., Karatay, E., Römer, G.R.B.E., Huis in't Veld, A.J., 2011. Laser-Induced Nanoscale Superhydrophobic Structures on Metal Surfaces. Langmuir 27, p. 8464–8469.

Jensen, D.A., Friedrich, L.M., Harris, L.J., Danyluk, M.D., Schaffner, D.W., 2013. Quantifying transfer rates of Salmonella and Escherichia coli O157:H7 between fresh-cut produce and common kitchen surfaces, Journal of Food Protection 76, p. 1530–1538.

Karickhoff, S.W., Bailey, G.W., 1973. Optical absorption spectra of clay minerals, Clays and Clay Miner 21, p. 59–70.

Kietzig, A.-M., Hatzikiriakos, S.G., Englezos, P., 2009. Patterned superhydrophobic metallic surfaces. Langmuir 25, p. 4821–4827.

Kietzig, A-M., Mirvakili, M.N., Kamal, S., Englezos, P., Hatzikiriakos, S.G., 2011. Laser-Patterned Super-Hydrophobic Pure Metallic Substrates: Cassie to Wenzel Wetting Transitions, Journal of Adhesion Science and Technology 25, p. 2789–2809.

Kumar, G., Prabhu, K.N., 2007. Review of non-reactive and reactive wetting of liquids on surfaces, Advances in Colloid and Interface Science. 133, p. 61–89.

Li, B., Logan, B.E., 2004. Bacterial adhesion to glass and metal-oxide surfaces. Colloids and Surfaces B: Biointerfaces 36, p. 81–90.

Nosonovsky, M., Bhushan, B., 2009. Superhydrophobic surfaces and emerging applications: Non-adhesion, energy, green engineering, Current Opinion in Colloid & Interface Science 14, p. 270–280.

Pou, J., Trillo, C., Soto, R., Doval, A.F., Boutinguiza, M., Lusquiños, F., Quintero, F., Pérez-Amor, M., 2003. Surface treatment of granite by high power diode laser, Journal of Laser Applications 15,p. 261–266.

Ragesh, P., Ganesh V.A., Nair, S.V., Nair, A.S., 2014. A review on "self-cleaning and multifunctional materials", Journal of Materials Chemistry A 2, p. 14773–14797.

Razi, S., Madanipour, K., Mollabashi, M., 2016. Laser surface texturing of 316L stainless steel in air and water: A method for increasing hydrophilicity via direct creation of microstructures, Optics & Laser Technology 80, p. 237–246.

Riveiro, A., Soto, R., Comesaña, R., Boutinguiza, M., del Val, J., Quintero, F., Lusquiños, F., Pou, J., 2012. Laser surface modification of PEEK, Applied Surface Science 258, p. 9437–9442.

Riveiro, A., Soto, R., del Val, J., Comesaña, R., Boutinguiza, M., Quintero, F., Lusquiños, F., Pou, J., 2014. Laser surface modification of ultra-high-molecular-weight polyethylene (UHMWPE) for biomedical applications, Applied Surface Science 302, p. 236–242.

Riveiro, A., Mejías, A., Soto, R., Quintero, F., del Val, J., Boutinguiza, M., Lusquiños, F., Pardo, J., Pou, J.,2016. CO2 laser cutting of natural granite, Optics & Laser Technology 76, p. 19–28.

Riveiro, A., Soto, R., del Val, J., Comesaña, R., Boutinguiza, M., Quintero, F., Lusquiños, F., Pou, J., 2016. Texturing of polypropylene (PP) with nanosecond lasers, Applied Surface Science 374, p. 379–386.

Rodrigues, J.D., Costa, D., Mascalchi, M., Osticioli, I., Siano, S., 2014. Laser ablation of iron-rich black films from exposed granite surfaces, Applied Physics A 117, p. 365–370.

Scott, E., Bloomfield, S.F., Barlow, C.G., 1982. An investigation of microbial contamination in the home, Journal of Hygiene 89, p. 279–293.

Stone Sector 2015, the international market of natural stone - News - IMM CARRARA, 2016. http://www.immcarrara.com/uk/IMM/elenco-news/stone-sector-2015-the-international-market-of-natural-.asp (accessed April, 2016).

Rukosuyev, M.V., Lee, J., Cho, S.J., Lim, G., Jun, M.B.G., 2014. One-step fabrication of superhydrophobic hierarchical structures by femtosecond laser ablation, Applied Surface Science 313, p. 411–417.

Ta, D.V., Dunn, A., Wasley, T.J., Kay, R.W., Stringer, J., Smith, P.J., Connaughton, C., Shephard, J.D., 2015, Nanosecond laser textured superhydrophobic metallic surfaces and their chemical sensing applications. Applied Surface Science 357, p. 248–254.

Vorobyev, A.Y., Guo, C., 2013. Direct femtosecond laser surface nano/microstructuring and its applications, Laser & Photonics Reviews 7, p. 385–407.

Wang, R., Bai, S., 2015. Wettability of laser micro-circle-dimpled SiC surfaces. Applied Surface Science 346, p. 107–110.

Wenzel, R.N., 1936. Resistance of solids surfaces to wetting by water, Industrial & Engineering Chemistry 28, p. 988–994.

Wu, B., Zhou, M., Li, J., Ye, X., Li, G., Cai, L., 2009. Superhydrophobic surfaces fabricated by microstructuring of stainless steel using a femtosecond laser. Applied Surface Science 256, p. 61–66.

Young, T., 1805. An Essay on the Cohesion of Fluids, Philosophical Transactions of the Royal Society B: Biological Sciences 95, p. 65–87.